INVESTIGATION OF UD HIBRIDE BASALT FIBER/EPOXY COMPOSITE MECHANICAL PROPERTIES DEPENDING ON LENGTH

Umesh Vavaliya[1], Ilgar Jafarli[1], Olga Kononova[1], Iveta Novakova[2], Riho Motlep[3]
[1]Riga Technical University, Latvia; [2]UiT the Arctic University of Norway, Norway;
[3]University of Tartu, Estonia
umesh-haribhai.vavaliya@rtu.lv, ilgar.jafarli@edu.rtu.lv, olga.kononova@rtu.lv,
iveta.novakova@uit.no, riho.motlep@ut.ee

Abstract. A basalt micro-fiber bundle (yarn), slightly twisted and impregnated by polymeric matrix with uniformly distributed within the matrix volume microscopical particles of oil shale ash (OSA) is used in textile reinforcement of a composite structure. Oil shale ash (OSA) is a powder, obtained in the combustion process, during generation of electricity at electrical power plants in Estonia. Polymeric matrix is epoxy resin. Mechanical properties of the hybrid composite - epoxy matrix (with OSA) reinforced by continuous basalt fibers depend significantly on the stress transfer and failure mechanisms occurring at the micro-fiber-matrix interface. The present work experimentally investigates the strength of such basalt fiber/epoxy (with OSA) composite rod, emphasizing its dependence on length. Composite samples were experimentally fabricated with 10 wt.% of OSA in polymeric matrix impregnated basalt micro-fiber bundles forming rods with a diameter of 0.13cm. Experimentally fabricated rods are with the length 1, 10 and 82 cm. The rods were tested by tension till rupture and the stochastic Weibull approach was used for rod strength statistical evaluation. The results revealed a scale effect, where shorter rods exhibited higher tensile strengths compared to longer rods, attributed to the lower probability of critical flaws in smaller volumes. The experimental strength data were analyzed using the two-parameter Weibull distribution. The shape parameter α ranged from 3.87 (82 cm) to 8.98 (10 cm), while the scale parameter β increased from 891 MPa (82 cm) to 1169 MPa (1 cm). These Weibull parameters quantify the length-dependent strength variability of the basalt fiber/epoxy composite rods, enabling stochastic modeling of the reinforcement fragmentation process when such rods are used in composite structures.

Keywords: SFFT, OSA, basalt fiber.

Introduction

Composite materials have been a subject of significant interest in various industries due to their potential to combine the best properties of different materials. One such composite that has gained attention is the basalt fiber/epoxy composite [1]. Basalt fibers are derived from volcanic basalt rock, a plentiful and naturally occurring material. The process of producing basalt fibers involves melting of the crushed basalt rock at around 1400 to 1700 degrees Celsius, followed by extrusion through platinum/rhodium bushings to manufacture continuous fibers. This process is environmentally friendly and results in a product that offers several beneficial properties [2]. Toorchi et al. [1] studied the impact behaviour and interlaminar shear strength of basalt fiber/epoxy composites with nano-ZrO2/graphene oxide hybrid fillers. Guler and Akbulut [2] examined the high-temperature resistance of geopolymer cement mortars reinforced with steel and basalt fibers. Khan et al. [3] investigated the use of basalt fibers in modified whisker-reinforced cementitious composites.

One of the key advantages of basalt fibers is their relatively high tensile strength compared to other fiber types. Tensile strength refers to the resistance of a material to breaking under tension. Basalt fibers exhibit a tensile strength that may be greater than that of E-glass fibers and is close to that of S-glass and aramid fibers [3]. This high tensile strength makes basalt fibers suitable for applications where strength is a critical requirement. In addition to high tensile strength, basalt fibers also offer slightly higher E-modulus (elastic modulus) than glass fibers (see Table 1), which is a measure of a material's stiffness. Materials with a high E-modulus do not deform easily under load, making them suitable for applications where rigidity is required. Basalt fibers also exhibit high abrasion strength, which means they can resist wear and tear, further enhancing their durability [4]. Another notable property of basalt fibers is their high temperature resistance. They can withstand temperatures up to 800 degrees Celsius without significant loss of properties [5]. This makes them suitable for applications where the material is expected to be exposed to high temperatures. Basalt fibers also offer excellent thermal and sound insulation properties. This makes them suitable for applications where insulation from heat or noise is required. For example, they can be used in the construction of buildings to provide thermal insulation and soundproofing [6].

Despite these promising properties, the use of basalt fibers in polymer composites presents certain challenges. One of the main challenges is achieving adequate interfacial adhesion between the basalt fibers and the polymer matrix. Poor adhesion can result in weak bonding between the fibers and the matrix, which can adversely affect the mechanical properties of the composite [7]. To improve this situation, various strategies have been explored, including the use of surface modification techniques and the incorporation of nano fillers, because the use of boron/epoxy composite macro-fibers looks as a promising approach for polymer and concrete structure [8-10; 11] reinforcement.

In this context, the present study aims to investigate the mechanical properties of unidirectional (UD) basalt fiber/epoxy composites, with a specific focus on the influence of fiber length. The study employs a unique approach, utilizing a basalt fiber bundle impregnated by a polymeric matrix with uniformly distributed microscopical particles of oil shale ash (OSA).

Oil shale ash (OSA) is a kind of ash obtained after combustion of oil shale (OS). OSA from Auvere Power plant (Estonia) was used in our experiments. The organic part of oil shale mainly consists of hydrocarbons. Oil shale ash from power plants was classified as hazardous material according to the Material safety data sheet for burnt oil shale enforced with the EC regulations No 1907/2006 and EU No 453/2010. But starting from 2018 oil shale ash is no longer classified as hazardous material [12; 13]. Addition of OSA is changing elastic properties of the matrix inside the macro-fiber. The mechanical properties of these composites are significantly influenced by the stress transfer through outer surface and failure mechanisms occurring at the fiber-matrix interface [10; 11; 14].

Previous studies have investigated the mechanical properties of basalt fiber-reinforced composites, but the influence of fiber length and the incorporation of fillers like OSA have not been explored enough.

Stochastic strength parameters of such composite rods (macro-fibers) are important for damage accumulation process evaluation in concretes reinforced by short and long composite macro-fibers. By experimental investigation the strength of the basalt fiber/epoxy composite rods, having different length, it is possible to obtain and analyse the macro-fibers rupture statistics in the concrete matrix and polymer matrix loaded composites [8; 10; 11; 15]. The present work aims to bridge this gap by conducting a comprehensive experimental and analytical study on the strength of basalt fiber/epoxy (with OSA) composite rods, emphasizing its dependence on length. The outcomes of this study are anticipated to contribute significantly to the understanding of basalt fiber/epoxy composite macrofiber mechanical properties during the macrofiber fragmentation process, which is crucial when such macrofibers are used as reinforcements in composite structures.

Materials and methods

The basalt micro-fibers used in this experiment were produced by the Deutsche Basalt Faser GmbH[15]. Macro-fiber consists of a micro-fiber bundle impregnated by epoxy resin with 10% OSA. The production process of basalt roving involves the assembly of a spinning cake into a roving. Basalt roving offers several advantages over other types of fibers. It exhibits a higher tensile strength compared to glass and polypropylene fibers, making it a more robust material for composite applications. Despite its superior strength, the basalt roving is more cost-effective than carbon fiber, making it a viable option for various applications. The properties of the basalt fiber are given in the table.

Table 1

Properties of basalt fibre [13]

Property	Fiber	Epoxy
Density	2.7 g·cm^{-3}	1.14 g·cm^{-3}
Poisson ratio	3.0	3.5
Linear tenacity	2500tex	-
Elastic modulus (E-modulus)	90-100 GPa	4 GPa
Tensile strength	3000-4000 MPa	30 MPa (Yield)

These fibers, when embedded in an epoxy resin matrix, form a composite material with improved mechanical properties. The epoxy resin serves as a binding agent, holding the fibers together and transferring load between them. However, the mechanical properties of the composite are not solely

dependent on the individual constituents but are significantly influenced by the interactions at the fiber-matrix interface.

A critical parameter in the study of composite materials is the fiber volume fraction, which represents the proportion of the total volume of the composite occupied by the fibers[16]. In the context of our hybrid basalt fiber/epoxy with OSA composite, the fiber volume fraction was calculated using the weights and densities of the fiber and the matrix. At the beginning epoxy resin was mixed with 10% by weight OSA powder [17]. Thirteen composite samples were prepared, each comprising basalt fiber yarns impregnated with epoxy (with OSA) resin. The composite fibers were uniformly cut to a length of 100 cm. Subsequently, the diameter and weight of each composite sample were measured to ascertain their physical properties. The average diameter of the 13 composite samples was found to be 0.127cm. Moreover, the collective average weight of the composite fibers (W_c) was determined to be 4.34 grams. To provide a comparative analysis, five samples of basalt fiber yarns of the same length were examined without epoxy impregnation, yielding an average weight (W_f) of 2.65 grams. To quantify the epoxy impregnation within the composite yarns, the weight of the epoxy resin with OSA was deduced by subtracting the average weight of the basalt yarns without epoxy (with OSA) impregnation from the average weight of the impregnated composite samples. All the calculations are given in Table 2.

Given the respective densities of epoxy (1.13 g·cm^{-3}) and basalt fiber yarn (2.7 g·cm^{-3}), the volume of the fiber (V_f) was calculated as the ratio of the weight of the basalt fiber yarn to ρ_f – the density of the fiber ($V_f = W_f / \rho_f$). Similarly, the volume of epoxy (V_m) within the composite samples was determined by dividing the difference in the weight between the composite samples and the basalt fiber yarns by ρ_m – the density of the epoxy (with OSA) [17] ($V_m = (W_c - W_f) / \rho_m$).

Table 2

Fiber volume fraction

Sample	**Composite weight, g** W_c	**Weight of epoxy, g** $W_c - W_f$	**Volume of matrix, g·cm^{-3}** V_m	**Volume of fiber, g·cm^{-3}** V_f	**Fiber volume fraction** $v_f = \frac{V_f}{V_m + V_f}$
Sample 1	4.66	2.01	1.77	0.98	0.35
Sample 2	4.31	1.66	1.46	0.98	0.40
Sample 3	4.47	1.82	1.61	0.98	0.37
Sample 4	4.31	1.66	1.46	0.98	0.40
Sample 5	4.72	2.07	1.83	0.98	0.34
Sample 6	4.23	1.58	1.39	0.98	0.41
Sample 7	3.9	1.25	1.10	0.98	0.47
Sample 8	4.62	1.97	1.74	0.98	0.36
Sample 9	4.09	1.44	1.27	0.98	0.43
Sample 10	4.24	1.59	1.40	0.98	0.41
Sample 11	4.52	1.87	1.65	0.98	0.37
Sample 12	4.15	1.50	1.32	0.98	0.42
Sample 13	4.24	1.59	1.40	0.98	0.41
Average	**4.34**	**1.69**	**1.49**	**0.98**	**~ 0.40**

Using these values, the fiber volume fraction was calculated to be approximately 40%. This value indicates that nearly half of the composite volume is occupied by the basalt fibers, highlighting their significant contribution to the composite overall mechanical properties.

Experiment

The composite fibers used in this experiment were pre-cut to a uniform length of 100 cm. These fibers were then further cut into three different lengths – 82 cm, 10 cm, and 1 cm – for the tensile tests. To ensure reliable results, at least eight composite samples were prepared for each fiber length. The composite fibers were carefully inserted into specially designed wooden tabs at each end. These tabs served as fixtures to securely hold the fibers in place during testing and were designed to fit into a standard tensile testing machine. After the fibers were inserted, the tabs were filled with epoxy resin to

secure the fibers in place. Figures 1a and 2 show the wooden tabs with the hybrid composite fibers inserted and numbered from 1 to 8.

This process was repeated for all three lengths of fibers – 82 cm, 10 cm, and 1 cm. The resulting samples were then ready for mechanical testing. By systematically varying the length of the composite fibers and subjecting them to standardized testing procedures, the experiment aimed to gain insights into how fiber length influences the overall mechanical behaviour of composite materials.

The tensile testing was performed using a Zwick-Roell Z150 tensile and compression testing machine [11]. The composite samples, prepared as described in the Sample Preparation section, were installed in the testing machine for the tensile tests. The tests were conducted according to the ASTM D3379-75 standard with a preload of 5 N and a test speed of 5 $mm \cdot min^{-1}$ or 8.33E-5 $m \cdot s^{-1}$. Figure 1b shows a single fiber attached for testing in the Zwick-Roell Z150 machine. This setup allowed for precise control over the testing conditions and ensured the reliability of the test results.

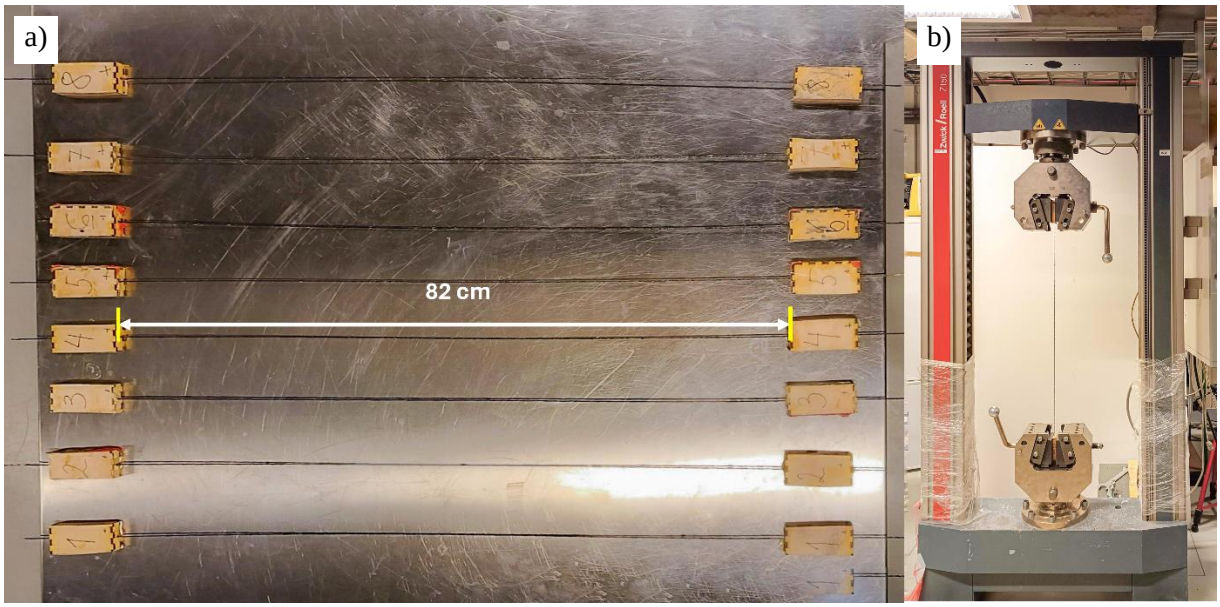

Fig. 1. **Composite fibers with tabs (a) and tensile testing experiment (b)**

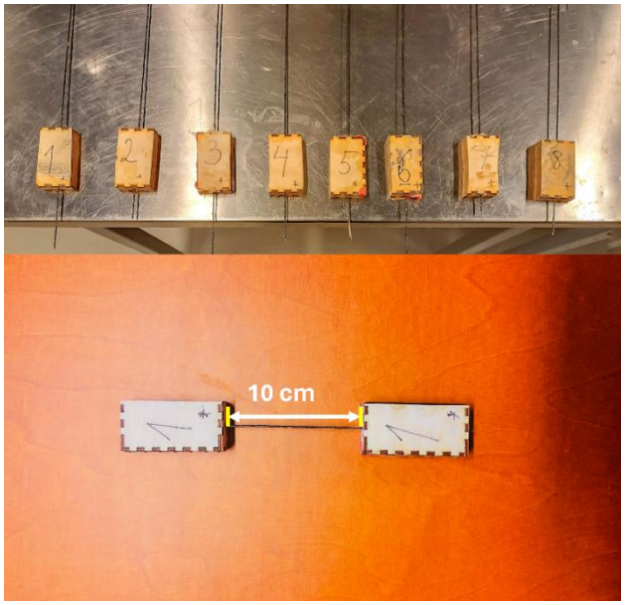

Fig. 2. **10 cm Samples with tabs**

Upon completion of the tensile tests on the hybrid composite fibers of varying lengths, we obtained the stress-strain data for each sample. The data graphical presentation (stress-strain curves) made by the testing machine computer for each of the fiber lengths – 82, 10 and 1 cm, is depicted in Fig. 3-5.

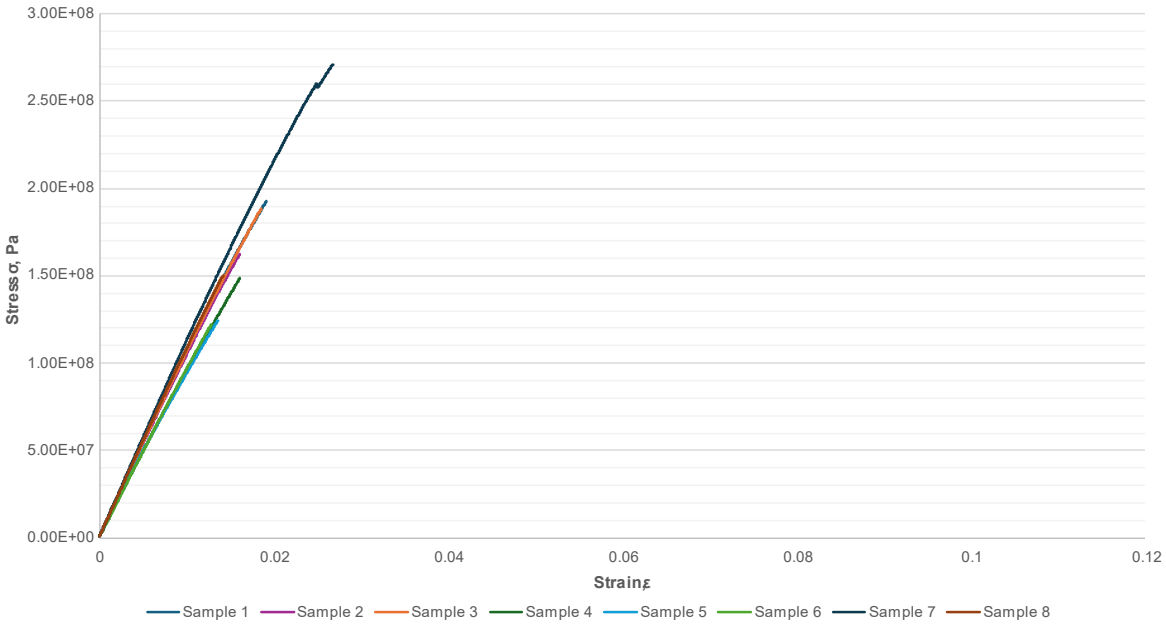

Fig. 3. **Stress Strain graph for 82 cm fiber**

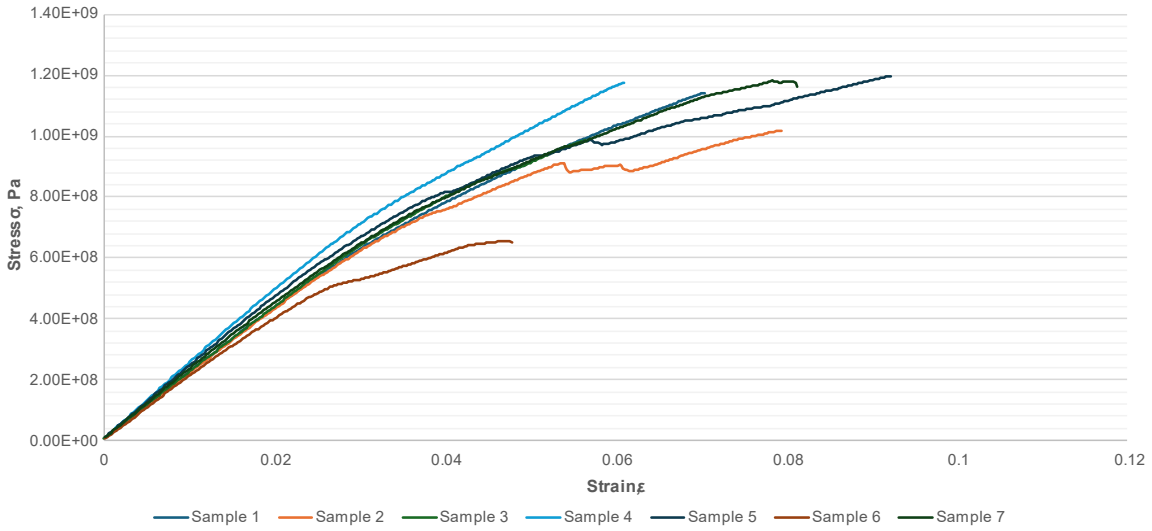

Fig. 4. **Stress Strain graph for 10 cm fiber**

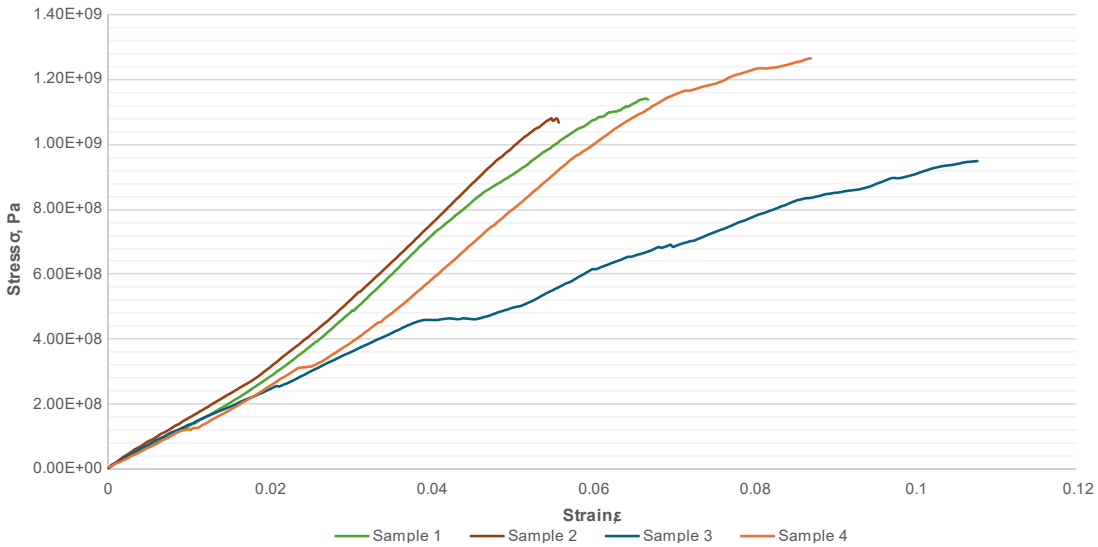

Fig. 5. **Stress Strain graph for 1 cm fiber**

The 1 cm macro-fiber exhibits a higher strength compared to the 82 cm long macro-fiber. This is a scale effect. The scale effect is easy to explain using the stochastic approach to the problem. "The stochastic approach" refers to the use of the probability theory and statistical methods to model the inherent variability and randomness in the strength properties of materials. In the case of fiber-reinforced composites, the strength is governed by the distribution of defects or flaws within the fibers and matrix [29]. The longer fibers may have a higher probability of containing a flaw that could act as an ultimate stress concentrator, leading to failure at lower stress levels. This is because the probability of a critical flaw existing within the volume of the material decreases as the size (in this case, length) of the sample decreases. The scale effect is governed by the lower tail (value) distribution in the set of strength distributions of different length macro-fibers.

Subsequently, we computed the mean strength values for macro-fibers having the same given length. The strength values for the macro-fibers are presented in Table 3.

Table 3

Macrofiber strength values in Pa

Macrofiber length	**82 cm**	**10 cm**	**1 cm**
Sample 1	5.77E+08	6.55E+08	9.50E+08
Sample 2	5.90E+08	9.85E+08	1.08E+09
Sample 3	7.07E+08	1.02E+09	1.14E+09
Sample 4	7.12E+08	1.14E+09	1.27E+09
Sample 5	7.70E+08	1.17E+09	-
Sample 6	8.93E+08	1.18E+09	-
Sample 7	9.13E+08	1.20E+09	-
Sample 8	1.28E+09	-	-
Mean	**8.05E+08**	**1.05E+09**	**1.11E+09**

From Table 3, the mean strength value for samples l = 82 cm long is 805 MPa, for samples l = 10 cm long is 1050 MPa and for samples l = 1 cm long is 1110 MPa.

Results and discussion

From the tensile test, we found the maximum stress value, which is able to carry every particular tested sample across all lengths of the tested samples. At the same time, for one particular sample it is the weakest crossection strength in the sample. One of the probabilistic distributions that describe distribution of lower values is the Weibull distribution [18-21].

Now we can observe the composite material matrix reinforced by reinforcement- hybrid macro-fibers. The strength of the composite is mainly dependent on the strength of its reinforcement. The variability in the strength of macro-fibers, in composite materials, we will model by macro-fibre crossection strength stochastic distribution, using for that the Weibull distribution. We can approximate the distribution of the strength of the composite and its reinforcement by the two parameter Weibull distribution.

$$P(\sigma) = 1 - \exp\left(\frac{l}{l_0}\left[\frac{\sigma}{\beta}\right]^{\alpha}\right), \tag{1}$$

where α, β are **"**shape**"** and **"**scale**"** numerical parameters;
l, l_0 – the macro-fiber length and reference length respectively;
σ – stress;
$P(\sigma)$ – strength probability for the sample having the gauge length equal to l.

In order to obtain the Weibull probability distribution curve, we need to find experimentally numerical values for **"**shape**"** factor α and **"**scale**"** factor β. To estimate the Weibull parameters for the basalt fiber/epoxy (wit 10% OSA) hybrid composite macro-fibers, the experimental data (fiber length and corresponding mean, over one-gauge length tested sample strength values) were utilized. The maximum stress values for each fiber length were arranged in ascending order, and ranks were assigned,

with the lowest strength value receiving a rank of 1, the next higher strength value receiving a rank of 2, and so on [22]. The probability of failure, P, was calculated using the median rank estimator [22]:

$$P = \frac{1-0.3}{n+0.4}, \tag{2}$$

where i – rank of the strength value;
n – total number of samples for the respective macro-fibers.

For instance, considering the 82 cm gauge length macro-fiber with a total of $n = 8$ samples, the probability of failure for the lowest strength value with a rank of 1 was calculated as

$$P = \frac{1-0.3}{8+0.4} = 0.0833\cdot$$

This process was repeated for each strength value across all gauge lengths of macro-fiber to obtain the corresponding P values. Next, the quantity ln(ln(1(1 – P)) was calculated for each strength value and plotted against ln(σ). The resulting data points were fitted with a linear regression. By plotting ln(ln(1(1 – P)) against ln(σ) the **"**shape**"** parameter α can be obtained from the slope of the linear fit, and the **"**scale**"** parameter β can be calculated from the intercept [22; 23]. The plot is given in Fig. 6-8.

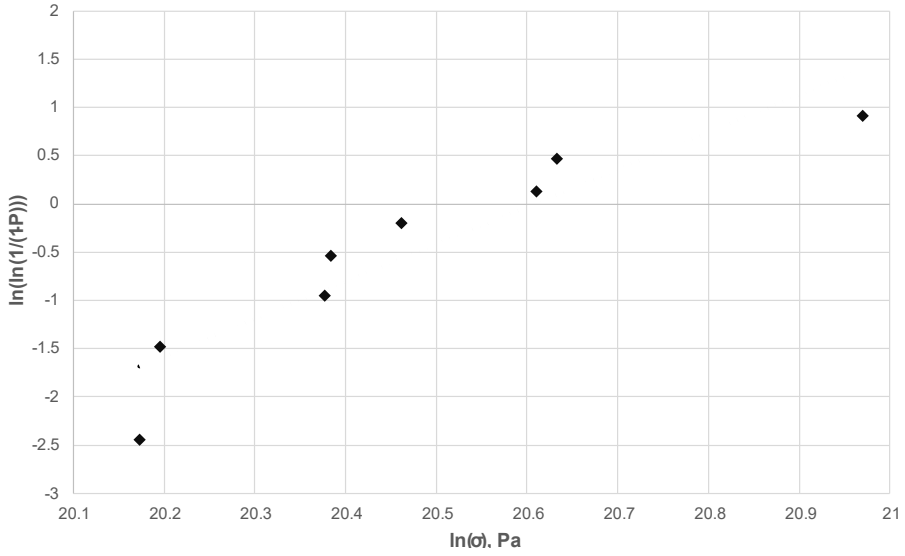

Fig. 6. **Gauge length – 82 cm test results on Weibull coordinates**

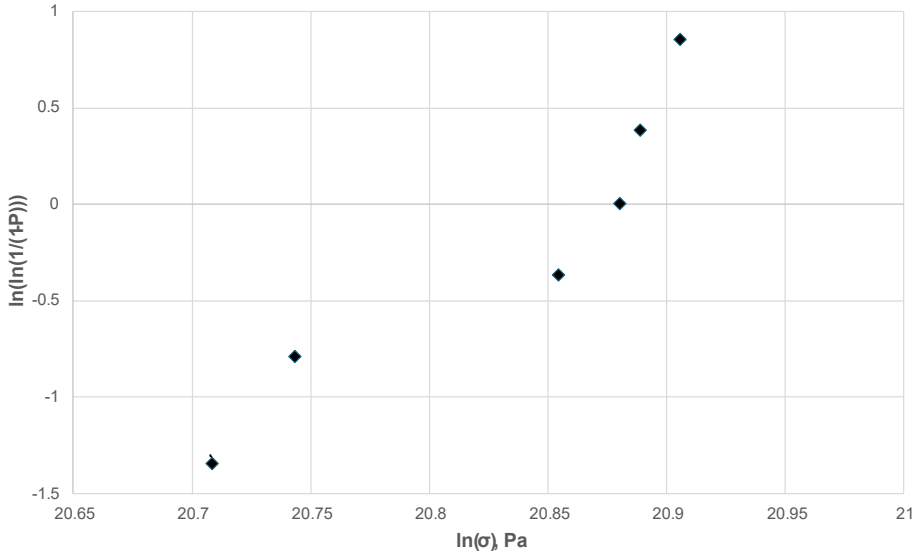

Fig. 7. **Gauge length – 10 cm test results on Weibull coordinates**

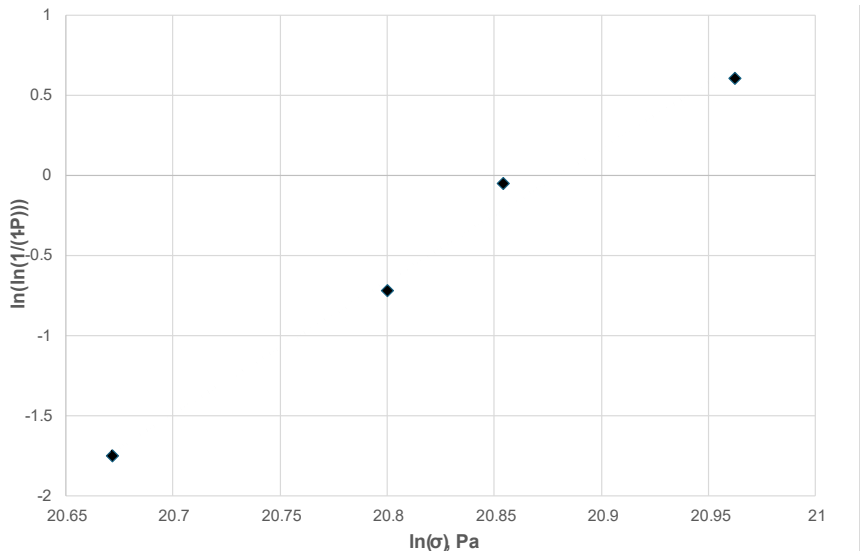

Fig. 8. **Gauge length – 1 cm test results on Weibull coordinates**

The obtained numerical values for Weibull distribution are shown in Table 4. In Table 5 are shown the **"**shape**"** parameter α and **"**scale**"** parameter β values obtained for single micro-fibers by different authors. Our macro-fiber consists of hundreds micro-fibers embedded in matrix.

Table 4

Obtained numerical values for Weibull distribution

Parameter	82 cm fiber	10 cm fiber	1 cm fiber	Average
Shape parameter (α)	3.872	8.976	8.299	7.05
Scale parameter β	891.09 MPa	1139.17 Mpa	1169.41 Mpa	1066.56 Mpa

Table 5

Weibull distribution parameters in literature

Test	Shape parameter, α	Scale parameter, β, GPa	Ref.
Carbon fiber T700 Sigle fiber test	3.23	4.19	[24]
Carbon fiber T700 Sigle fiber test	5.6	5.4	[25]
Carbon fiber T700 Sigle fiber test	4	6.2	[26]
E-glass fibres, Sigle fiber test	5.43	3.03	[22]
Cellulose fibers Cordenka 700 Super 3 Sigle fiber test	10.8	1.03	[23]
Basalt fibers BF1 sigle fiber test	31.63	1.94	[27]
Basalt fibers BF1 sigle fiber test	28.6	1.80	[28]

Conclusions

The overarching purpose of this research was to experimentally investigate and quantify the scale effects on the tensile strength of hybrid basalt fiber/epoxy composite reinforcements containing oil shale ash (OSA) fillers. While previous studies have examined the mechanical properties of basalt fiber composites, the novelty of the present work lies in its systematic exploration of the influence of the reinforcement length, as well as the unique approach of incorporating OSA particles within the epoxy matrix impregnating the basalt fiber bundles. The tensile stress-strain results clearly demonstrate the scale effect on strength. The shorter 1 cm rods exhibited significantly higher strengths compared to the longer 82 cm rods. This trend of increasing strength with decreasing length is an expected phenomenon in fiber-reinforced composites and is attributed to the lower probability of encountering critical defects or flaws over smaller material volumes. While the individual strength values may seem abstract, they provide crucial data points for establishing the strength distributions as a function of rod length.

By analysing this data within the framework of the Weibull statistical strength theory, the pivotal scale and shape parameters (β and α) could be determined. These Weibull parameters quantitatively

capture the length-dependence of the strength variability. Such quantification is vital for developing stochastic models to predict damage initiation, fiber fracture, and fragmentation processes when such reinforcing fiber rods are used in larger-scale composite structures under mechanical loading.

The multi-scale experimental data generated in this study provides a comprehensive set of inputs for strength models aimed at optimizing the design and performance of basalt fiber reinforced polymer and concrete composites for diverse structural applications. While further studies may be required to investigate other factors like fiber-matrix interfaces, the current experiments establish a systematic methodology to characterize the fundamental scale effects on the composite reinforcement strength.

Acknowledgements

The authors acknowledge financial support from the Baltic Research Programme Project No. EEA-RESEARCH-165 “Innovation in concrete design for hazardous waste management applications” under the EEA Grant of Iceland, Liechtenstein and Norway Project Contract No. EEZ/BPP/VIAA/2021/6.

Author contributions

Contribution of each author. Conceptualization, O.K., I.N.; methodology, O.K., I.N. and R.M.; software, O.K. and U.V.; validation, O.K., I.J. and U. V.; formal analysis, R.M. and O.K.; investigation, I.J.; and U.V.; writing – original draft preparation, U.V., O.K.; writing – review and editing, U.V., O.K. and I.N.

All authors have read and agreed to the published version of the manuscript.

References

[1] Toorchi D., Khosravi H., Tohidlou E. “Synergistic effect of nano-ZrO2/graphene oxide hybrid system on the high-velocity impact behavior and interlaminar shear strength of basalt fiber/epoxy composite,” Journal of Industrial Textiles, vol. 51, no. 2, Aug. 2021, pp. 277-296, DOI: 10.1177/1528083719879922.

[2] Guler S., Akbulut Z. F. “The single and hybrid use of steel and basalt fibers on high-temperature resistance of sustainable ultra-high performance geopolymer cement mortars,” Structural Concrete, vol. 24, no. 2, Apr. 2023, pp. 2402-2419, DOI: 10.1002/SUCO.202201026.

[3] Khan M., Cao M., Ai H., Hussain A. “Basalt Fibers in Modified Whisker Reinforced Cementitious Composites,” Periodica polytechnica. Civil engineering, vol. 66, no. 2, Mar. 2022, pp. 344-354, DOI: 10.3311/PPCI.18965.

[4] Hu S., Li T., Su Z., Liu D. “Research on suitable strength, elastic modulus and abrasion resistance of Ti-Zr-Nb medium entropy alloys (MEAs) for implant adaptation,” Intermetallics (Barking), vol. 140, Jan. 2022, DOI: 10.1016/J.INTERMET.2021.107401.

[5] Tang Y., Yao H., Xu W., Zhu L., Zhang Y., Jiang Z. “Side-Chain-Type High Dielectric-Constant Dipolar Polyimides with Temperature Resistance,” Macromol Rapid Commun, vol. 44, no. 2, p. 2200639, Jan. 2023, DOI: 10.1002/MARC.202200639.

[6] Bumanis G. et al., “Thermal and Sound Insulation Properties of Recycled Expanded Polystyrene Granule and Gypsum Composites,” Recycling 2023, Vol. 8, Page 19, vol. 8, no. 1, p. 19, Feb. 2023, DOI: 10.3390/RECYCLING8010019.

[7] Khare E., Holten-Andersen N., Buehler M. J. “Transition-metal coordinate bonds for bioinspired macromolecules with tunable mechanical properties,” Nat Rev Mater, vol. 6, no. 5, May 2021, pp. 421-436, DOI: 10.1038/S41578-020-00270-Z.

[8] Macanovskis A., Lukasenoks A., Krasnikovs A., Stonys R., Lusis V. Composite fibers in concretes with various strengths, ACI Materials Journal, 115 (5), 2018, pp. 647-652.

[9] Lusis V., Annamaneni K.K., Kononova O., Korjakins A., Lasenko I., Karunamoorthy R.K., Krasnikovs A. Experimental Study and Modelling on the Structural Response of Fiber Reinforced Concrete Beams Open Access, Applied Sciences (Switzerland) Vol. 12, Iss.19, October 2022, Article number 9492,

[10] Varna J., Krasnikovs A. Transverse cracks in cross-ply laminates 2. Stiffness degradation Mechanics of Composite Materials, 34 (2), 1998, pp. 153-170, DOI 10.1007/BF02256035

[11] Kharkova G., Kononova O., Krasnikovs A., (...) Machanovskis E., Dzelzitis K. Elastic properties of cotton fabric based polymer composites, Engineering for Rural Development, 10th International

Scientific Conference on Engineering for Rural Development 26-27 May 2011 pp. 402-407, ISSN 16915976

[12] Uibu M., Tamm K., Velts-Jänes O., Kallaste P., Kuusik R., Kallas J. Utilization of oil shale combustion wastes for PCC production: Quantifying the kinetics of Ca(OH)2 and CaSO4·2H2O dissolution in aqueous systems. Fuel Processing Technology, 140 (2015), pp. 156-164. DOI: 10.1016/j.fuproc.2015.09.010

[13] Trikkel A., Kuusik R., Martins A., Pihu T., Stencel J. M. Utilization of Estonian oil shale semicoke. Fuel Processing Technology, 89(8), (2008), pp. 756-763. DOI: 10.1016/j.fuproc.2008.01.010

[14] Jiang H., Kamdem D. P., , B. Bezubic, Ruede P. "Mechanical properties of poly(vinyl chloride)/wood flour/glass fiber hybrid composites," Journal of Vinyl and Additive Technology, vol. 9, no. 3, Sep. 2003, pp. 138-145, DOI: 10.1002/VNL.10075.

[15] "Basalt Roving - Deutsche Basalt Faser." Accessed: Mar. 14, 2024. [online] [11.02.2024] Available: https://www.deutsche-basalt-faser.de/en/products/basalt-roving/

[16] Jasper B., Coenen J. W., Riesch J., Höschen T., Bram M., Linsmeier C. "Powder Metallurgical Tungsten Fiber-Reinforced Tungsten," Materials Science Forum, vol. 825-826, 2015, pp. 125-133, DOI: 10.4028/WWW.SCIENTIFIC.NET/MSF.825-826.125.

[17] Jafarli I., Mačanovskis A., Gjerløw E. and Vaišnoras M. Mechanical Properties Study of Epoxy and Concrete Based Composite Materials Reinforced with Oil Shale Ash Engineering for Rural Development, 10th International Scientific Conference on Engineering for Rural Development 22-24 May 2024(to be published).

[18] Ermolenko AF. Scale effect of strength in tensile loading unidirectional reinforcing elements. Mech Comp Mater 1986;22(1), pp. 31-36.

[19] Sebastien Joannes, Faisal Islam, Lucien Laiarinandrasana Uncertainty in fibre strength characterisation due to uncertainty in measurement and sampling randomness Applied Composite Materials (2020), 27, pp. 165-184, DOI: 10.1007/s10443-020-09803-9

[20] Tamuzh VP, Korabel'nikov Y G, Rashkovan IA, Karklin'sh AA, Gorbatkina Y A, Zakharova Y T. Determination of scale dependence of strength of fibrous fillers and evaluation of their adhesion to the matrix, based on results of tests of elementary fibers in a polymer block. Mech. Comp. Mater. 1991;27(4), pp. 413-418

[21] Phoenix SL. Probabilistic strength analysis of fibre bundle structures. Fibre Sci. and Technol. 1974;7, pp. 15-31.

[22] Andersons J., Joffe R., Hojo M., Ochiai S. Glass fibre strength distribution determined by common experimental methods, Composites Science and Technology, 62 (2002), pp. 131-145

[23] Andersons J., E. J. Sparninsh, Joffe R., Wallstrom L. Strength distribution of elementary flax fibres, Composites Science and Technology 65 (2005), pp. 693-702 DOI: 10.1016/j.compscitech.2004.10.001

[24] Joannes S., Islam F., Laiarinandrasana L. Uncertainty in fibre strength characterisation due to uncertainty in measurement and sampling randomness Applied Composite Materials (2020), 27, pp. 165-184, DOI: 10.1007/s10443-020-09803-9

[25] Feih S., Manatpon K., Mathys Z., Gibson A. G., Mouritz A. P. Strength degradation of glass fibers at high temperatures, Journal of Materials Science 44 (2) (2009), pp. 392-400. DOI:10.1007/s10853-008-3140-x.

[26] Deng S., Ye L., Mai Y.-W., Liu H.-Y. Evaluation of fibre tensile strength and fibre/matrix adhesion using single fibre fragmentation tests, Composites Part A: Applied Science and Manufacturing 29 (4) (1998), pp. 423 - 434. DOI: 10.1016/S1359-835X(97)00094-8.

[27] Ralph C., Lemoine P., Summerscales J., Archer E. and McIlhagger A. Relationships among the chemical, mechanical and geometrical properties of basalt fibers Textile Research Journal 2018 DOI: 10.1177/0040517518805376

[28] Ralph C., Lemoine P., Summerscales J., Archer E., McIlhagger A. Relationships among the chemical, mechanical and geometrical properties of basalt fibers Textile Research Journal 2018 DOI: 10.1177/0040517518805376

[29] Phoenix S. L., Schwartz P., Robinson H. H. "Statistics for the strength and lifetime in creep-rupture of model carbon/epoxy composites," Composites Science and Technology, vol. 32, no. 2, Jan. 1988, pp. 81-120, DOI: 10.1016/0266-3538(88)90001-2.